HEAVY ION PHYSICS IN ATLAS*

Krzysztof W. Woźniak

on behalf of the ATLAS Collaboration

The H. Niewodniczański Institute of Nuclear Physics, Polish Academy of Sciences
Radzikowskiego 152, 31-342 Kraków, Poland

(Received April 24, 2013)

During the operation in the years 2009–2013, the Large Hadron Collider (LHC) was delivering not only collisions of proton beams, but also Pb+Pb collisions and p+Pb collisions, at the center of mass energy $\sqrt{s_{NN}} = 2.76$ TeV and $\sqrt{s_{NN}} = 5.02$ TeV, respectively. In this contribution, selected recent results of the analyzes of heavy ion collisions from the ATLAS experiment are presented.

DOI:10.5506/APhysPolB.44.1677
PACS numbers: 25.75.–q

1. Introduction

The primary goal of the experiments at the Large Hadron Collider is a study of proton–proton collisions at extreme energies providing opportunities to test the Standard Model and to search for signs of new phenomena. Results of recent analyses focused on the most fundamental interactions, including those obtained using the ATLAS detector [1], are discussed in several contributions to these proceedings. Studies of heavy ion collisions explore much more complicated systems created in the volumes much larger than the size of the proton under the conditions of extreme energy density. Such conditions are similar to those at an early phase of the Universe evolution, when the matter was in the state of strongly interacting Quark-Gluon Plasma (QGP). Results of nuclei collisions depend on the size of the volume and its shape, which are directly connected with the smallest distance of the nuclei centers during the collision. Commonly, centrality of the nuclei collisions is denoted by the percentage of the cross section (starting

* Presented at the Cracow Epiphany Conference on the Physics After the First Phase of the LHC, Kraków, Poland, January 7–9, 2013.

from the most central events) or is characterized by the number of nucleons participating in inelastic interactions, $N_{\rm part}$, or by the number of binary nucleon–nucleon collisions, $N_{\rm coll}$. Collective effects, which are sensitive to properties of the interaction volume and can be studied in azimuthal correlations, are described in Section 2. Interactions of energetic partons created inside the colliding system with the medium are analyzed in Section 3. The recent results for proton–nucleus collisions are briefly presented in Section 4 and the summary of the ATLAS heavy ion results is included in Section 5.

2. Collective flow in Pb+Pb collisions

In the collisions of nuclei, only some fraction of nucleons are actively participating in the interactions. Their number and geometrical positions are determined by the overlap of the nuclei. The strongly interacting QGP appears thus in a volume with elongated shape resembling an almond. Asymmetry of this volume induces different pressure gradients which later lead to enhanced emission of particles, called flow, in the direction of the shorter axis, which coincides with the event reaction plane. As the nucleon positions may vary from event to event, the shape of the initial interaction volume fluctuates. All these effects modify the azimuthal angle distribution, which can conveniently be expanded in Fourier series

$$\frac{dN}{d\phi} \sim 1 + 2\sum_{n=1}^{\infty} v_n(p_{\rm T}, \eta) \cos\left(n(\phi - \Phi_n)\right) , \tag{1}$$

where the azimuthal angle of a particle and of the reaction plane are denoted by ϕ and Φ_n, respectively, and the parameters of the expansion v_n depend on particles transverse momentum, $p_{\rm T}$, and pseudorapidity, η.

The dominating parameter in the Fourier expansion is v_2, called elliptic flow, which reflects the almond-like shape of nuclei overlap. As it will be shown later, higher order harmonics are related to the fluctuations of nuclei positions. The flow harmonics, v_n, can be measured with the *event plane method* as well as from two-particle correlations in azimuthal angle (*two-particle correlations method*) [2]. In the latter approach, in place of harmonics $v_n = \langle\cos(n(\phi - \Phi_n))\rangle$ parameters $v_{n,n} = \langle\cos(n(\phi_a - \phi_b))\rangle$ appear in the expansion formula [2]. When the correlations originate from collective flow, v_n and $v_{n,n}$ parameters fulfill the relation

$$v_{n,n}\left(p_{\rm T}^a, p_{\rm T}^b\right) = v_n\left(p_{\rm T}^a\right) v_n\left(p_{\rm T}^b\right) . \tag{2}$$

The flow harmonics can be also calculated using the cumulants from $2k$-particle correlations (*cumulant method* [3]).

In Fig. 1 the values of elliptic flow, v_2, are presented as a function of pseudorapidity for several centrality intervals [4]. The largest values are observed for semi-peripheral collision (30–60%). In Fig. 1 only a weak dependence on η is visible in the limited η range available in the ATLAS detector. The PHOBOS experiment at RHIC observed for $|\eta|$ a triangular shape [5]. However, when ATLAS and PHOBOS results are transformed to the rest frame of one of the colliding nuclei (Fig. 2), the trend in η dependence observed at the RHIC and the LHC is consistent and suggests that extended longitudinal scaling is, at least approximately, valid up to the LHC energies.

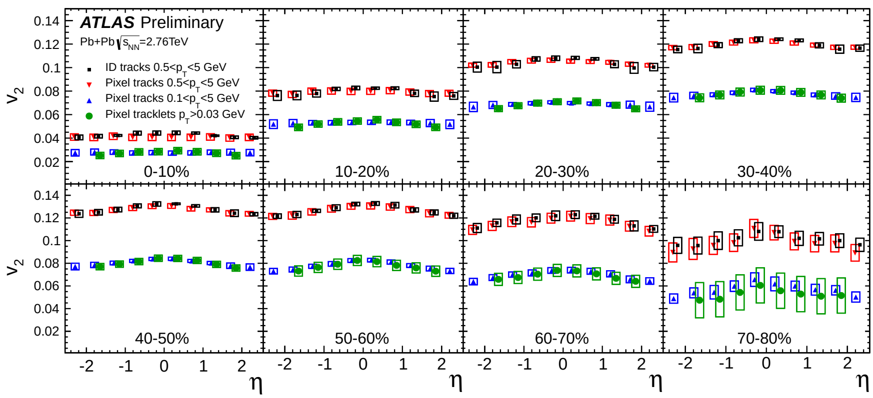

Fig. 1. Pseudorapidity, η, dependence of v_2 integrated over p_{T} for different tracking methods and different low-p_{T} thresholds in centrality bins, as described in the legend [4].

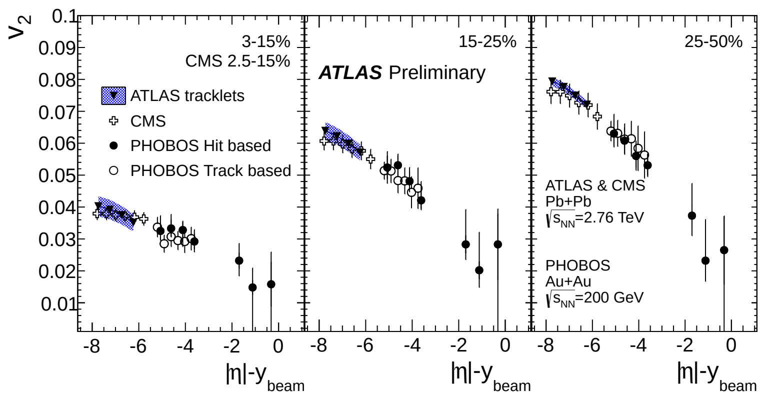

Fig. 2. Integrated v_2 as a function of $|\eta|-y_{\mathrm{beam}}$ for three centrality bins, as indicated on the plots, measured by the ATLAS and CMS LHC experiments for Pb+Pb collisions at 2.76 TeV [4] and by the PHOBOS experiment at RHIC for Au+Au collisions at 200 GeV [5].

The values of v_2 are the largest of all harmonics for almost all centralities with the exception of the most central collisions (0–5%), where v_2 becomes comparable to v_3 and v_4 (see Fig. 3). With this exception and for other centralities the absolute value of v_n decreases with n (for n = 2–6). In Fig. 4 the dependence of flow harmonics on particle transverse momentum is shown [2]. The hydrodynamic expansion of the interaction volume is reflected in a rapid increase of v_n values up to $p_{\mathrm{T}} \sim$ 2–3 GeV, while a slower decrease and, finally, very weak dependence at large p_{T} values can be connected with coalescence and jet quenching processes. The shape of all harmonics stays very similar for different centrality classes.

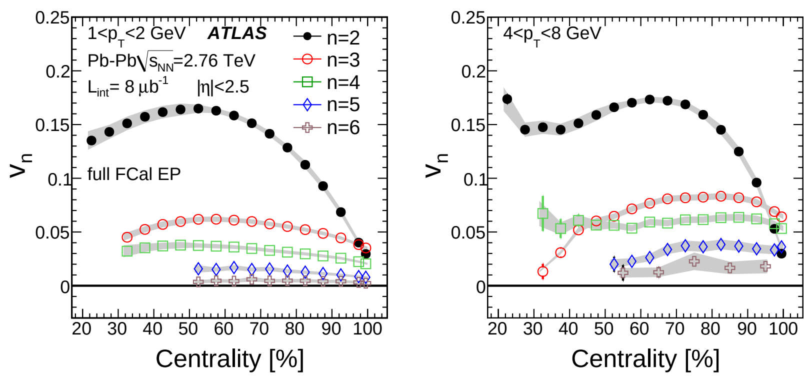

Fig. 3. Flow harmonics v_n obtained from the *event plane method* [2] as a function of collision centrality for two p_{T} ranges. Systematic errors are shown as shaded bands.

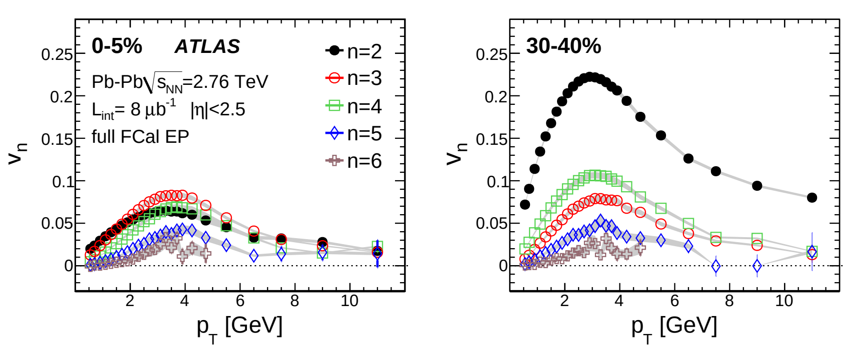

Fig. 4. Flow harmonics v_n obtained from the *event plane method* [2] as a function of p_{T} for the most central (0–5%) collisions (left) and semi central (30–40%) collisions (right). Systematic errors are shown as shaded bands.

The ATLAS detector allows to study the flow harmonics on the event-by-event basis [6]. In Fig. 5 probability distributions of three flow harmonics are shown. v_3 and v_4 probability distributions are consistent with a 2D Gaussian distribution indicating that they are mostly due to the fluctuations in the nucleon positions. For v_2 distribution, a Gaussian fit is valid only for the most central collisions, while in other centrality bins v_2 distributions are narrower.

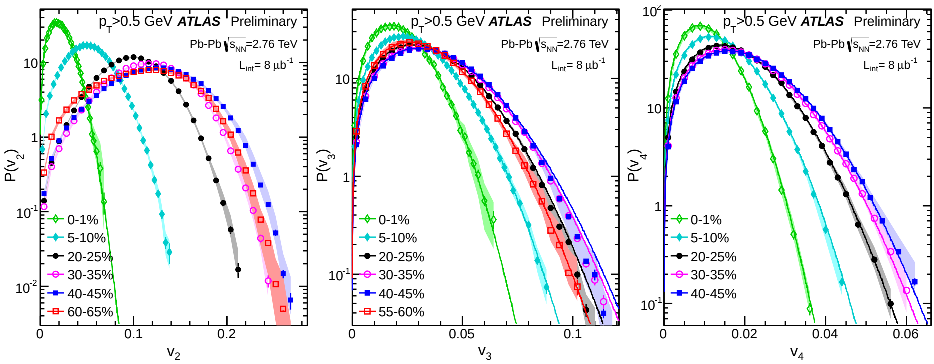

Fig. 5. The probablity distributions of flow harmonics v_2, v_3 and v_4 obtained on the event-by-event basis [6]. The errors bars are statistical uncertainties, and the shaded bands are uncertainties on the v_n shape.

Finally, interesting results provides the comparison of elliptic flow obtained from the *event plane method*, v_2, and $2k$*-particle cumulant methods*, $v_2\{2k\}$. The flow harmonics v_2 and $v_2\{2\}$ are larger than $v_2\{4\}$ as shown

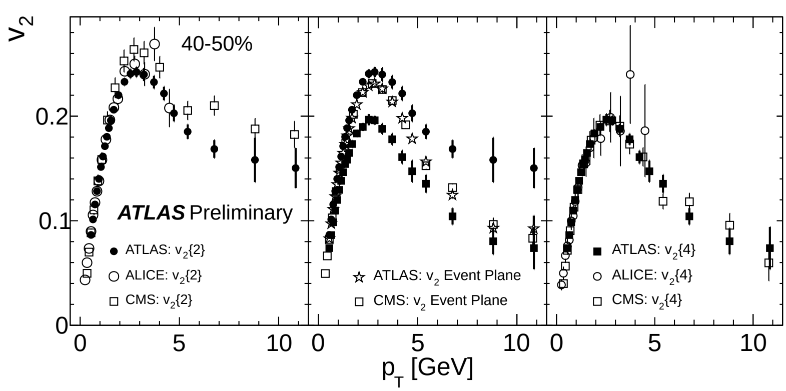

Fig. 6. Comparison of elliptic flow from the *event plane metod*, v_2, and *cumulant metods*, $v_2\{2\}$ and $v_2\{4\}$, for the centrality bin 40–50% at mid-rapidity [3] from ATLAS, CMS and ALICE experiments.

in Fig. 6. This suggests that non-flow two-particle correlations influence the first two observables, while they are canceled in $v_2\{4\}$ [3].

3. Interactions of energetic partons and particles with the QGP

The most spectacular new feature observed in the heavy-ion collisions at the LHC is the disappearance of jets in the most central Pb+Pb collisions [7]. Unlike in the $p+p$ interactions, where almost always at least 2 jets are produced simultaneously, in Pb+Pb collisions quite frequently only one highly energetic jet is found. This is explained by strong interactions of partons, even those most energetic, with the dense medium created in the collision. Fraction of the energy lost by such parton depends on the path length in the strongly interacting matter and thus increases with collision centrality.

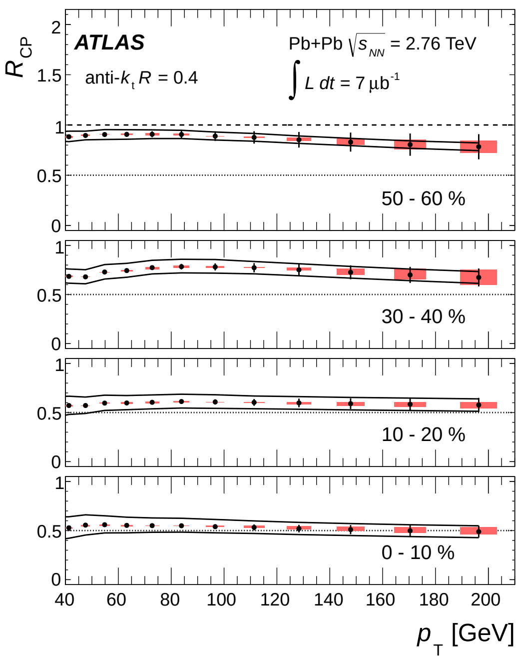

Fig. 7. R_{CP} values (Eq. (3)) as a function of jet p_{T} for jet size $R = 0.4$ in four bins of collision centrality calculated with respect to peripheral sample 60–80%. Three sources of uncertainties are presented: statistical (error bars), partially correlated unfolding regularization systematics (shaded boxes) and fully correlated systematic errors (solid lines). The horizontal width of the systematic error band is added for clarity of presentation only. Dotted lines indicate $R_{\mathrm{CP}} = 0.5$, and the dashed lines on the top panels indicate $R_{\mathrm{CP}} = 1$ [9].

Quantitative description of jet (or particle) suppression is frequently provided by the ratio R_{CP}, in which the yields are normalized to one nucleon–nucleon binary collision

$$R_{\mathrm{CP}} = \frac{\frac{1}{N_{\mathrm{coll}}^{\mathrm{centr}}} \frac{1}{N_{\mathrm{ev}}^{\mathrm{centr}}} \frac{dN_{\mathrm{jet}}^{\mathrm{centr}}}{dp_{\mathrm{T}}}}{\frac{1}{N_{\mathrm{coll}}^{\mathrm{periph}}} \frac{1}{N_{\mathrm{ev}}^{\mathrm{periph}}} \frac{dN_{\mathrm{jet}}^{\mathrm{periph}}}{dp_{\mathrm{T}}}}, \tag{3}$$

where in the nominator and denominator values for varying centrality and values for appropriately selected peripheral sample are used, respectively. In Fig. 7 the dependence of R_{CP} on jet transverse momentum is presented. In the most central events the jet yields are about 2 times smaller than in peripheral collisions, but the dependence on jet momentum is very weak.

In order to verify that the jet suppression depends on the path length of the parton in the medium, the ratio of the jet yields for different azimuthal angles, $R_{\Delta\phi}$, can be studied [8]

$$R_{\Delta\phi} \;=\; \frac{\frac{d^2 N_{\mathrm{jet}}}{dp_{\mathrm{T}} d(\Delta\phi)}(\Delta\phi)}{\frac{d^2 N_{\mathrm{jet}}}{dp_{\mathrm{T}} d(\Delta\phi)}(0 < \Delta\phi < \pi/8)}, \tag{4}$$

where $\Delta\phi$ denotes the angle of the jet relative to the event plane. As the path length in the event plane is the shortest, we expect the largest jet yields in this direction. In this case, the values of $R_{\Delta\phi}$ should be always smaller than 1. This expectation is confirmed in Fig. 8, where the values of $R_{\Delta\phi}$

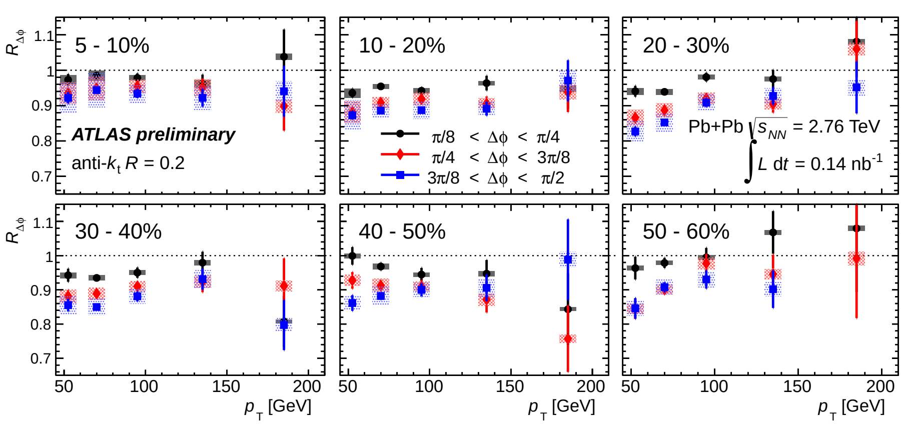

Fig. 8. $R_{\Delta\phi}$ as a function of p_{T} for three bins of $\Delta\phi$ calculated relative to the $0 < \Delta\phi < \pi/8$ bin for different centrality bins. Error bars show statistical uncertainties, shaded boxes indicate systematic uncertainties [8].

are usually the lowest for the direction perpendicular to the event plane ($3\pi/8 < \Delta\phi < \pi/2$). Although the statistical and systematic errors are too large to draw definite conclusions, the suppression in the perpendicular direction is visibly smaller in the central collision (0–20%) than in more peripheral — again consistently with the difference in the elongation of the interaction volume.

The interactions of partons in the QGP affect not only the relative yieds of jets, but also their fragmentation into observed particles. A convenient tool for a study of jet fragmentation provides the change of the jet size parameter R used in the anti-$k_{\rm t}$ algorithm of jet reconstruction [9]. In the analysis of Pb+Pb data it was varied from 0.2 to 0.5, and appropriate values of $R_{\rm CP}^{0.2}$ to $R_{\rm CP}^{0.5}$ were calculated. Jets obtained for lower R values are characterized by stronger suppression. More quantitatively it is shown in Fig. 9, where the values of $R_{\rm CP}^{R}$ for $R = 0.3, 0.4$ and 0.5 are divided by that for $R = 0.2$. The values of $R_{\rm CP}^{R}/R_{\rm CP}^{0.2}$ are larger than 1 for the jets with the large radii R, especially for $p_{\rm T} < 100$ GeV. This observation indicates a "widening" of jets, which however is not sufficient to account for all energy lost by the parton in the QGP volume. An exact energy balance shows that the jet energy is transfered also to the particles with low momenta and emitted at larger angles from the jet axis [10].

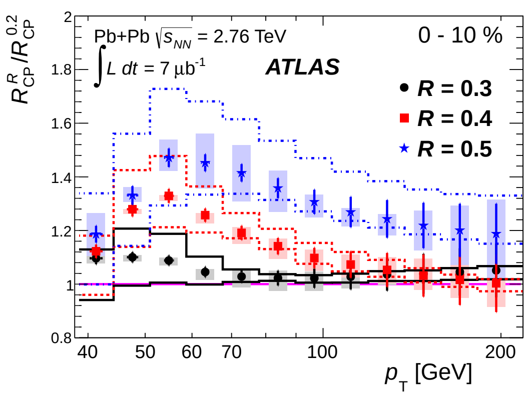

Fig. 9. Ratios of $R_{\rm CP}^{R}$ values to $R_{\rm CP}^{R=0.2}$ for $R = 0.3$, 0.4 and 0.5 (where R is the jet size parameter), as a function of $p_{\rm T}$ in the 0–10% centrality bin. Three sources of uncertainties are presented: statistical (error bars), partially correlated systematic errors (shaded boxes) and fully correlated systematic errors (lines) [9].

A more detail study of jet fragmentation using the particle longitudinal momentum fraction, $z = p_{\rm T}^{\rm ch}/p_{\rm T}^{\rm jet}\cos(\Delta R)$, is presented in Fig. 10 [11]. The ratio of the distribution $D(z)$ for several centralities to that for the most peripheral collisions, $R_{D(z)} = D(z)_{\rm centr}/D(z)_{60-80\%}$, is close to 1 at large z, drops up to 15% at intermediate z values $(0.05 < z < 0.2)$ and increases for $z < 0.05$. These results do not support theoretical models with radiative energy loss in the medium, which predict a suppression of particle yields at large z.

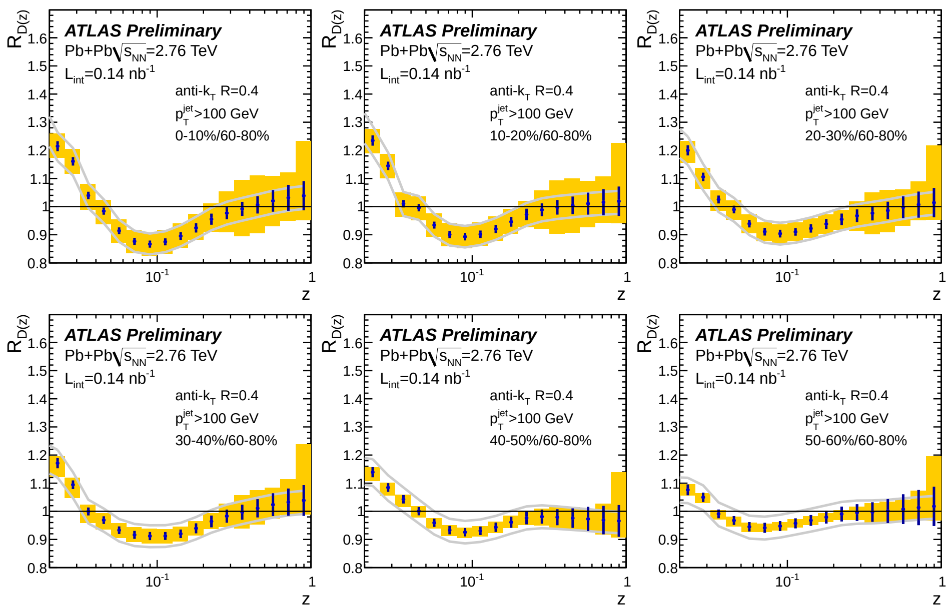

Fig. 10. Ratios of $R_{D(z)}$ for six bins in collision centrality to those in peripheral (60–80%) collisions, $D(z)_{\mathrm{centr}}/D(z)_{60-80\%}$, for $R = 0.4$ jets. The error bars on the data points indicate statistical uncertainties while the shaded bands indicate systematic uncertainties that are uncorrelated or partially correlated between points. The solid lines indicate systematic uncertainties that are 100% correlated between points[11].

Interesting results are provided by studies of jets correlated with prompt photons or Z bosons. Prompt photons originate from quark–gluon Compton scattering $qg \to q\gamma$ or quark–antiquark annihilation $q\bar{q} \to g\gamma$. In the analysis it is necessary to remove the contribution from dijet events in which a high energy photon is created in the fragmentation of one of the jets. Such events can be efficiently rejected by placing a limit on the additional energy registered near the photon in a cone $\sqrt{(\Delta\eta)^2 + (\Delta\phi)^2} < R_{\mathrm{iso}} = 0.3$ [12]. As the photons do not interact with the QGP, the ratio of the transverse momentum of the associated jet to the transverse momentum of the photon, $x_J = p_{\mathrm{T}}^{\mathrm{jet}}/p_{\mathrm{T}}^{\gamma}$, provides a measure of the energy lost by the parton in the strongly interacting matter. In Fig. 11 the *per photon* normalized distribution of x_J obtained from Pb+Pb data and from PHYTIA simulations overlaid with data events are shown. In the peripheral events, both distributions are compatible (similar shape and overall integral). In more central events, the distribution for the data is shifting towards smaller x_J and the overall integral decreases, while the results from reconstructed PHYTIA simulations have no significant centrality dependence.

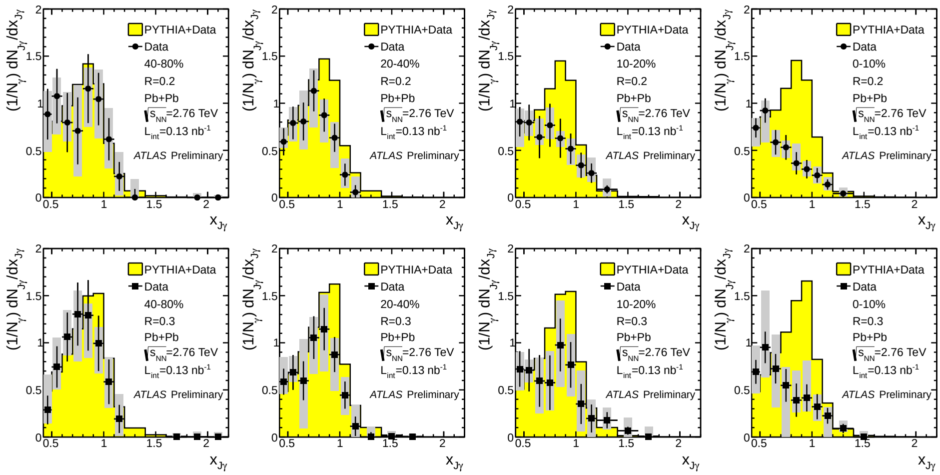

Fig. 11. Distributions of $dN_{J\gamma}/dx_{J\gamma}$ as a function of $x_{J\gamma}$ from lead–lead data (closed symbols) compared with PHYTIA truth jet/true photon distributions (grey/yellow histogram), for simulated events (embedded into underlying data events). The rows represent different reconstructed jet radii (respectively $R = 0.2$ and $R = 0.3$) and the columns — different centralities. The error bars represent statistical errors, while the grey bands indicate the systematic uncertainties [12].

The background from dijet events is negligible in another study: analysis of energies of a jet and Z bosons created in the same hard scattering. This type of correlation provides even more clear measure of the energy lost by the jet, but such signal is very rare and after all necessary cuts only 36 events were found in the full Pb+Pb data sample, corresponding to about 0.15 nb^{-1}, collected in 2011 [13]. However, even with so few events it is possible to calculate the mean value of the ratio $p_{\mathrm{T}}^{\mathrm{jet}}/p_{\mathrm{T}}^{Z}$, which clearly shows effects of jet suppression. Also the fraction of events with a Z boson and a jet among all events with Z boson shown in Fig. 12 is lower than that expected from the reconstructed PHYTIA events embedded in the real events.

The presented so far studies of jet suppression were performed for jets originating mostly from light quarks or gluons. There are, however, theoretical predictions suggesting that interactions of quarks with Quark-Gluon Plasma depend on their mass. This can be tested using reconstructed muons,

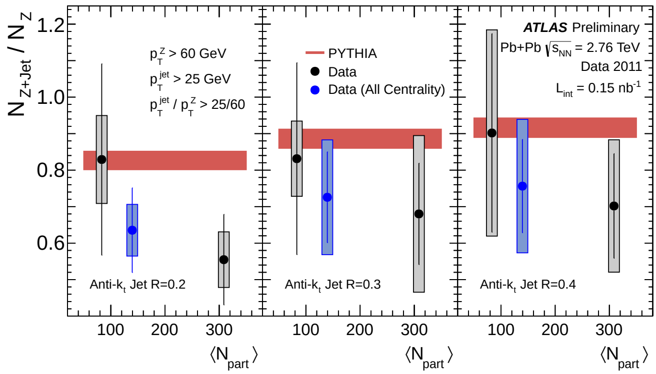

Fig. 12. The fraction of events with a Z boson ($p_T^Z > 60$ GeV) that also have a jet reconstructed ($p_T^{\text{jet}} > 25$ GeV, $p_T^{\text{jet}}/p_T^Z > 25/60$) as a function of N_{part}, for three jet cone sizes. Error bars represent statistical uncertainties, and shaded boxes, systematic uncertainties. The PHYTIA results (without any jet energy loss) are shown as bands, width of which represents their uncertainties [13].

in the $4 < p_T < 14$ GeV range, which originate predominantly from heavy flavor decays [14]. The calculated muon R_{CP} values indicate that the muons yields in the selected p_T range, and thus the yields of b quarks, are about 2.5 smaller in the most central collisions (0–10%) than in the peripheral events (60–80%). In Fig. 13 we can also see that there is no evidence of the p_T dependence of this suppression. The muon R_{CP} values are close to the corresponding R_{CP} for jets, but within comparable p_T range are higher than the R_{CP} for charged hadrons.

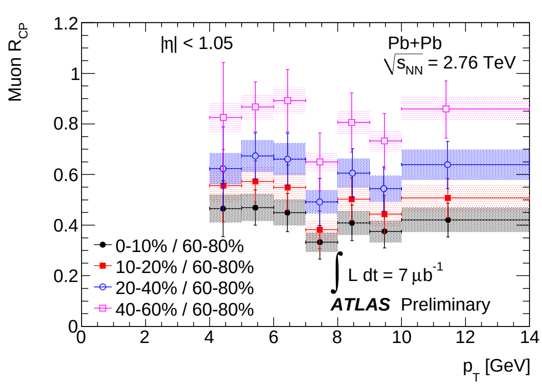

Fig. 13. Muon R_{CP} as a function of p_T for four centrality bins. The error bars include both statistical and uncorrelated systematic uncertainties, while the shaded boxes represent systematic uncertainties, which are fully correlated between p_T bins [14].

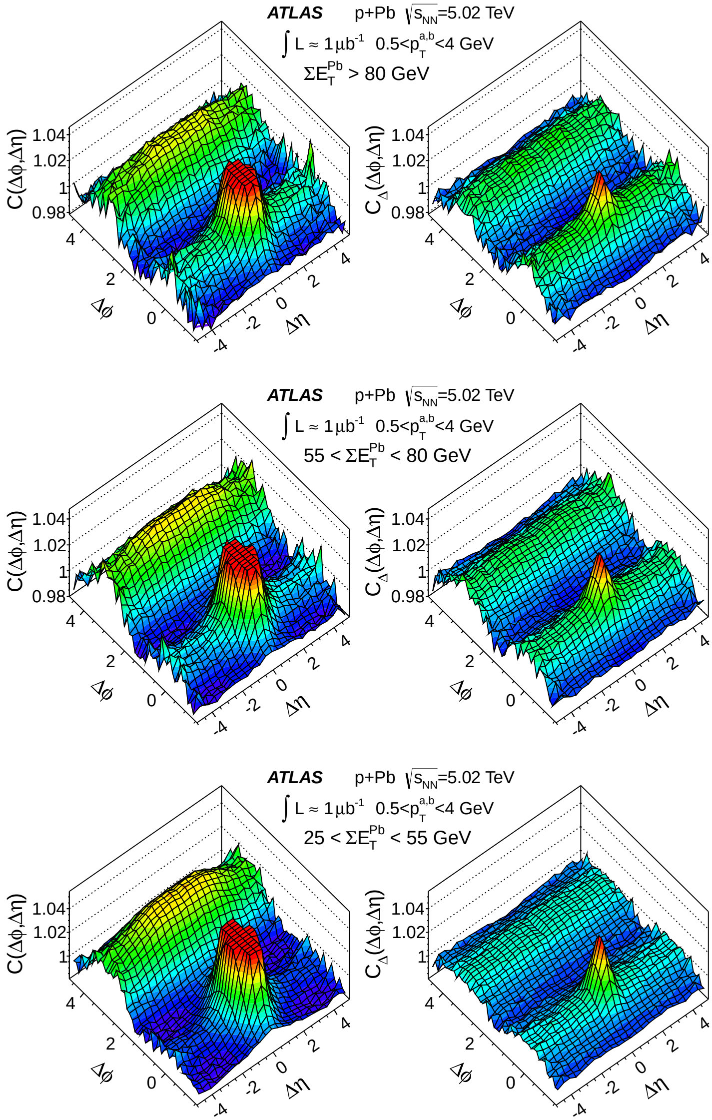

Fig. 14. Two-dimensional correlation function, $C(\Delta\phi, \Delta\eta)$, without (left) and with (right) subtraction of recoil contribution in events with $\sum E_{\mathrm{T}}^{\mathrm{Pb}} > 80$ GeV (top) $55 < \sum E_{\mathrm{T}}^{\mathrm{Pb}} < 80$ GeV (middle) and $25 < \sum E_{\mathrm{T}}^{\mathrm{Pb}} < 55$ GeV for $0.5 < p_{\mathrm{T}}^{a,b} < 4$ GeV. The recoil contribution is removed via a simple subtraction of the 2-D per-trigger yield distribution in a given $\sum E_{\mathrm{T}}^{\mathrm{Pb}}$ class via a simple subtraction of the yield in the peripheral class of $\sum E_{\mathrm{T}}^{\mathrm{Pb}} < 20$ GeV [15].

4. Long range azimuthal correlations in p+Pb collisions

The p+Pb collisions were first delivered by the LHC in September 2012 and then for a longer time in January 2013. The data from the first period were sufficient to perform the first ATLAS analysis for this new colliding system, focused on the two-particle correlations [16]. In the elementary proton–proton interaction, the 2D correlation in $\Delta\eta$ and $\Delta\phi$ features a peak at $\Delta\eta \approx 0$, $\Delta\phi \approx 0$ (from resonances and jets) and a broader correlation at $\Delta\phi \approx \pi$ extending also to large $|\Delta\eta|$ (recoil contribution resulting from dijets and momentum conservation effects). In the $p+p$ events with very large multiplicities, the correlation at $\Delta\phi \approx 0$ extends also to larger $|\Delta\eta|$ forming a "ridge" [17].

Similar "ridge" was also found in the ATLAS analysis of the correlations in p+Pb data [16]. In this case, events can be divided into centrality classes determined using the signals in the Forward Calorimeters, but only from the part in the direction of Pb fragmentation. In the peripheral collisions ($\sum E_{\mathrm{T}}^{\mathrm{Pb}} < 20$ GeV), the two-particle correlation has similar features as this for inclusive $p+p$ interactions. In more central collisions (larger $\sum E_{\mathrm{T}}^{\mathrm{Pb}}$), the correlation at $\Delta\phi \approx 0$ and large $|\Delta\eta|$ becomes stronger (left column in Fig. 14 [15]). In order to remove recoil contribution, the 2D correlation obtained for peripheral events was subtracted from the 2D correlations found for more central samples. Resulting 2D distributions are shown as plots at the right-hand side in Fig. 14. For all centralities considered, a similar $\cos(2\Delta\phi)$ modulation is observed at $|\Delta\eta| > 2$, but with the amplitude increasing with the centrality of the collision. More details on azimuthal correlations in p+Pb collisions are presented in another contribution to these proceedings [18].

5. Summary

Studies of the Pb+Pb collisions in the ATLAS experiment revealed several important properties of the Quark-Gluon Plasma. Strong interactions in the medium allow to preserve the initial geometry of the overlap of nuclei, which is then reflected in the azimuthal correlations. ATLAS has measured parameters of the Fourier decomposition (harmonics) v_n, for $n = 1, \ldots, 6$, in a wide pseudorapidity range, $|\eta| < 2.5$, and starting from very low momenta, $p_{\mathrm{T}} > 0.03$ GeV. The flow harmonics were calculated also from two-particle correlations and using cumulants in order to estimate the contributions from non-flow effects. Calculations of harmonics on the event-by-event basis were used to quantify the flow fluctuations.

Strong interactions of energetic partons and particles with the medium result in suppression of their yields, relative to elementary proton–proton or peripheral nucleus–nucleus collisions. Jets are suppressed by a factor of 2 in the most central collisions. The jet suppression is the smallest when parton is emitted in the event plane and increases in the perpendicular direction, indicating the dependence on the parton path length in the strongly interacting medium. Interactions of partons in the QGP lead to widening of the reconstructed jets in more central collisions. There is no significant difference between jets from light quarks and those from b quarks, as indicated by analysis of muon yields. In contrary, there is no evidence of suppression of photons and Z bosons, which do not interact with the medium. It is most clearly visible when the momentum of these particles is compared with the momentum of the associated jets, with the latter shifted to lower values in central Pb+Pb collisions. Such measurements are thus suitable to estimate the parton energy loss in the QGP.

The studies of p+Pb collisions allow to observed nuclear effects, which are not related to the QGP formation. Recent ATLAS analysis reveals long range azimuthal correlations, called "ridge", which increase with the centrality of the collision and resemble the flow observed in Pb+Pb collisions.

This work was supported in part by the National Science Center grant DEC-2011/03/B/ST/02631 and by PL-Grid Infrastructure.

REFERENCES

[1] ATLAS Collaboration, *JINST* **3**, S08003 (2008).
[2] ATLAS Collaboration, *Phys. Rev* **C86**, 014907 (2012).
[3] ATLAS Collaboration, ATLAS-CONF-2012-118.
[4] ATLAS Collaboration, ATLAS-CONF-2012-117.
[5] PHOBOS Collaboration, *Phys. Rev. Lett.* **94**, 122303 (2005).
[6] ATLAS Collaboration, ATLAS-CONF-2012-114.
[7] ATLAS Collaboration, *Phys. Rev. Lett.* **105**, 252303 (2010).
[8] ATLAS Collaboration, ATLAS-CONF-2012-116.
[9] ATLAS Collaboration, *Phys. Lett.* **B719**, 220 (2013).
[10] CMS Collaboration, *Phys. Rev.* **C84**, 024906 (2011).
[11] ATLAS Collaboration, ATLAS-CONF-2012-115.
[12] ATLAS Collaboration, ATLAS-CONF-2012-121.
[13] ATLAS Collaboration, ATLAS-CONF-2011-119.
[14] ATLAS Collaboration, ATLAS-CONF-2012-050.
[15] ATLAS Collaboration, `https://atlas.web.cern.ch/Atlas/GROUPS/PHYSICS/PAPERS/HION-2012-13`, additional auxiliary plots.
[16] ATLAS Collaboration, `arXiv:1212.5198 [hep-ex]`.
[17] CMS Collaboration, *J. High Energy Phys.* **09**, 091 (2010).
[18] B. Żabiński *et al.* [ATLAS Collaboration], *Acta Phys. Pol. B* **44**, 1691 (2013), this issue.